SIMPLE MODEL FOR ENERGY AND FORCE CHARACTERISTICS OF METALLIC NANOCONTACTS

V.V. POGOSOV[1,2], V.P. KURBATSKY[1], D.P. KOTLYAROV[1], A. KIEJNA[2]

UDC 539.2:538.915

[1]Department of Microelectronics, Zaporizhzhya National Technical University
(Zaporizhzhya 69064, Ukraine; e-mail: vpogosov@zstu.edu.ua),

[2]Institute of Experimental Physics, University of Wrocław
(Wrocław 50-204, Poland)

The quantum size oscillations of the energetic properties and the elongation force of gold slabs and wires isolated and in a contact with electrodes are calculated in a free-electron model. A simple relation between the Fermi energy and the square-potential-well depth is used and tested for low-dimensional systems. It is shown that considering the electron subsystem of a slab (or wire) in a contact as an open one, the contact acts like a sort of electron pump which sucks or pumps out electrons from the sample. The effect of the contact potential difference (CPD) on oscillations of the elastic force is considered. The calculated amplitudes of the force oscillations are in a qualitative agreement with those observed experimentally.

Introduction

Recent experimental investigations of gold point-contacts by using the atomic force microscope [1] have demonstrated a violation of the Hooke and Ohm laws: a deformation of the contact leads to a coherent stepwise variation of the conductance and force. A theoretical interpretation of these observations for a deformed nanowire was given in the framework of the simple free-electron models [2—7]. The energy picture of a nanocontact is more complicated, however, than that adopted in [2—6]. Firstly, in the previous considerations, CPD [8] was not taken into account. Second, the metallic contact changes its dimensionality with variation of the sample-cantilever distance. At first, its shape is rather similar to a slab, to resemble a wire at the moment of rupture [9, 10]. Thus, we have to do with a transformation of the $2D$ open electron system into a $1D$ one. The purpose of this work is to investigate the limiting cases of this transition. We study the size dependence of the work function, ionization potential, and elastic force of an isolated quantum slab and a wire that are inserted between two electrodes to form a contact. We begin with consideration of the energetics of an isolated sample. The results are exploited later to determine the CPD for a sample connected with electrodes.

In order to trace analytically the effect of dimensionality on the energy and force properties, one needs a simple model relating mutually the Fermi energy, work function, and potential barrier. We consider a rectangular sample of the volume $V = a \times a \times L$, where L denotes the dimension along the x-axis. The inequalities $a \gg L$ and $a \ll L$ correspond to the geometry of a slab and a wire, respectively. The consideration of these two asymptotic limits which simulate the early and late phases of elongation, allows us to trace the evolution of the energy and force characteristics of the $2D$ and $1D$ metallic structures.

We have assumed that the energetics of a finite system of bounded electrons can be described by a square potential well of the width L (slab) or a (wire) and the depth $U < 0$,

$$-U(E_{\mathrm{F}}) = W(E_{\mathrm{F}}) + E_{\mathrm{F}}, \qquad (1)$$

where W is the work function and E_{F} is the Fermi energy of a finite sample.

We recall that the potential well of the depth U of a metal sphere shows size oscillations [11]. The Fermi energy of a metal film also has size oscillations [12]. Due to an expansion of the chemical potential of a spherical cluster of radius R, $\mu = \mu_0 + \mu_1/R$, in powers of the inverse radius [13], we pay attention on the inequality

$$W = W_0 - \frac{\mu_1}{R} < W_0. \tag{2}$$

The criterion $W < W_0$ (the subscript zero labels the quantities for a semi-infinite metal) for one-dimensional systems was introduced by us [14] to check the correct size dependence of the $U(E_{\rm F})$ (by means $E_{\rm F}(L)$). In order to determine the size oscillations in the potential well depth $U(E_{\rm F})$, we have employed a simple expression for $W_0(E_{\rm F0})$ provided by [15]. The latter is based on the concept of the image force action [16, 17] and a spontaneous polarization of metallic plasma, to determine the distance from the classical metal surface, at which the image force begins to act (see also [18] and references therein),

$$W_0(E_{\rm F0}) = \frac{B}{r_s^{3/2} E_{\rm F0}^{1/2}}, \quad \text{(a.u.)} \tag{3}$$

where B is the adjusting parameter and r_{s0} is the average distance between electrons in the bulk, $B = 0.3721$ a.u. and $r_s = 3.01$ is the Bohr radius for gold.

Adapting the result for low-dimensional systems, we replace $W_0(E_{\rm F0})$ by $W(E_{\rm F})$ and suppose $W \to W_0 = 4.30$ eV [19] as $L \to \infty$ [14]. In order to get a qualitative agreement of the calculated force with experimental data, we have to assume that Au is monovalent [2, 3, 6].

1. Basic Relations for an Isolated Specimen

For $2D$ and $1D$ metallic systems, the allowed energy levels (the electron kinetic energies) form a quasi-continuum [20],

$$E_{n_{xyz}} = E_{n_x} + E_{n_y} + E_{n_z} = \frac{\hbar^2}{2m}(k_{n_x}^2 + k_{n_y}^2 + k_{n_z}^2).$$

For an infinitely deep potential well of width a (the shape is a cube), this expression reduces to $E_{n_{xyz}} = \hbar^2\pi^2 n_{xyz}^2/(2ma^2)$ with $n_{xyz}^2 = n_x^2 + n_y^2 + n_z^2$.

For simplicity, we assume that the wave vector components are the solutions of the transcendental equations for a square potential well:

$$k_n M = n\pi - 2\arcsin(k_n/k^0), \tag{4}$$

where $n = 1, 2, 3, \ldots$, and $n = n_x$ for $M = L$ and $n = n_y, n_z$ for $M = a$, $\hbar k^0 = \sqrt{-2mU}$. One gets two relations of identical form, to determine k_{n_y} and k_{n_z}. The inequalities $\max\{n_y, n_z\} \gg \max\{n_x\}$ for a slab and $\max\{n_y, n_z\} \ll \max\{n_x\}$ for a wire correspond to the highest occupied level.

The density of electron states, $D(E)$, is defined by the sum $\sum_{n_{xyz}} \delta(E - E_{n_{xyz}})$ over the allowed states. Replacing the three-dimensional summation in the k-space by integration over k_y and k_z (or over k_x) and summation over n_x (or over n_y and n_z), we get

$$D(E) = \frac{m}{\pi L\hbar^2} n_E, \tag{5}$$

and

$$D(E) = \frac{L}{V}\sqrt{\frac{2m}{\pi^2\hbar^2}} \sum_{n_y, n_z}^{+} (E - E_{n_y} - E_{n_z})^{-1/2} \tag{6}$$

for a finite slab (or a wire, respectively).

In Eq. (5) for a slab, n_E is the integer part of a number,

$$n_E = \left[\frac{kL + 2\arcsin(k/k^0)}{\pi}\right], \tag{7}$$

where $\hbar k = \sqrt{2mE}$.

In Eq. (6) for a wire, the plus sign in the limit of summation indicates that n_y and n_z run from 1 to the maximum value, for which the expression under the square root is positive.

Subsequently, the total number of electrons in a slab is given by

$$N = \frac{a^2 m}{\pi\hbar^2} \sum_{n_x=1}^{n_F} (E_{\rm F} - E_{n_x}), \tag{8}$$

where $n_{\rm F}$ is the number of the highest occupied subband and $n_{\rm F}$ equals n_E in Eq. (7) with the change $k \to k_{\rm F}$.

The total number of electrons in a wire is given by

$$N = 2L\sqrt{\frac{2m}{\pi^2\hbar^2}} \sum_{n_y, n_z}^{+} (E_{\rm F} - E_{n_y} - E_{n_z})^{1/2}. \tag{9}$$

Here, $N = \overline{n}V$, where $\overline{n} = 3/4\pi r_{s0}^3$ is the electron density in the bulk of the semi-infinite metal.

Discussing the effect of dimensionality and charging, it is useful to analyze the ionization potential which is a well-defined quantity for an arbitrary size of a specimen [21, 22]. The ionization potential (IP) which is defined as a work needed to remove an electron from a neutral metallic specimen can be expressed as

$$\text{IP} = W + \frac{e^2}{2C}, \tag{10}$$

where C is the capacitance of the specimen. It should be mentioned that W_0 and IP are the experimentally measured quantities, while W has mainly a methodical sense because it can be measured only in the limit of $C \to \infty$. An extended thin slab or a wire of infinite length has an infinite capacitance, $C \to \infty$. Therefore, IP $\to$ W. Equation (10) can be interpreted as the effect of charging on the work function of the neutral finite specimen. It should be noted that the size correction in $W(L)$ which is similar to that of the spherical cluster (see Eq.(2)) competes with the term $e^2/2C$. Since it is impossible to derive an analytic expression for the rectangular specimen, in order to estimate the monotonic size dependence of IP, we apply the well-known formula for the capacitance C of a disk of width L and of a needle of length L [23].

Solving the set of Eqs. (4) and (8) or (9), by using (1) and adapted Eq. (3), one can determine the Fermi energy E_F and subband energies for a given L under condition $V =$ constant. Consequently, one gets the work function W, as a function of the Fermi energy of a finite specimen.

The elastic elongation force acting on a finite sample is given by $F = -dE_t/dL$, where E_t is the total energy of the specimen. Neglecting the temperature effects in the adiabatic approximation, we have $E_t = -K$ from the virial theorem, which means that the energy of a bound electron-ion system is negative [14, 24]. (The virial and stress theorems for the electron-ion system of a solid metal were formulated in [25]. Consequently,

$$F = \frac{dK}{dL}. \tag{11}$$

In (11), we take into account the potential energy of the electron-ion system. This gives a plus sign in front of K (an opposite sign appeared in [2, 3, 6], where the simplest model of nanowire was exploited). The plus sign follows from the application of the virial theorem.

The total kinetic energy of electrons is given by the expressions

$$K = \frac{a^2}{2\pi^2}\frac{\hbar^2}{2m}\sum_{k_{n_x}}\int_0^{\sqrt{k_{\rm F}^2-k_{n_x}^2}}(\kappa^2+k_{n_x}^2)2\pi\kappa d\kappa =$$

$$= \frac{a^2 m}{2\hbar^2}\sum_{n_x=1}^{n_{\rm F}}(E_{\rm F}^2 - E_{n_x}^2), \tag{12}$$

and

$$K = \frac{2L}{3}\sqrt{\frac{2m}{\pi^2\hbar^2}}\sum_{n_y,n_z}^{+}(E_{\rm F}-E_{n_y}-E_{n_z})^{1/2}\times$$

$$\times(E_{\rm F}+2E_{n_y}+2E_{n_z}), \tag{13}$$

for an isolated slab and a wire, respectively.

2. The Effect of a "Point" Contact

When a specimen is inserted in a contact between the reservoirs, its electron subsystem has to be considered as an open one under the condition $W(L) = W_0$, where W and W_0 are the work functions for an isolated specimen and reservoirs, respectively. Due to CPD, $\delta\phi$, the electroneutrality of the specimen breaks down and δN electrons from the electron subsystem are transferred into reservoirs. In order to determined $\delta\phi$, one can imagine a simple energy cycle, in which electronic charges are transferred from a specimen to infinity and then into electrodes. By expressing the IP of the specimen charged by $+e\delta N$ in a form similar to that for charged spherical metal clusters [26, 27], we have

$$\text{IP} = E_{N-\delta N-\Delta} - E_{N-\delta N} =$$

$$= W\Delta + \frac{e^2}{2C}[(\delta N+\Delta)^2 - \delta N^2], \tag{14}$$

where $-e\Delta$ is a part of the electronic charge which leaves the charged specimen. The electron affinity of this electronic charge transferred to reservoirs is $EA = W_0\Delta$. The equilibrium condition IP $- EA = 0$ leads to

$$W_0 - W - \frac{e^2}{2C}(2\delta N+\Delta) = 0. \tag{15}$$

It should be noted that the magnitude of Δ can be infinitesimally small (non-integer), because the residual electron can be transferred only partially in a contact (an open system). That is, there is a finite probability that it could be found both in a sample and in a reservoir. Thus, we can ascribe a continuous value to δN. We also suppose that C of a rectangular specimen appearing in Eq. (14) corresponds to the total capacitance C_c of both contacts. This is justified by the fact that, near the two faces of a specimen, the surplus positive charges have a similar surface distribution both in the case of real ionization of an isolated specimen and for a specimen in contact. (This situation is similar to that encountered in

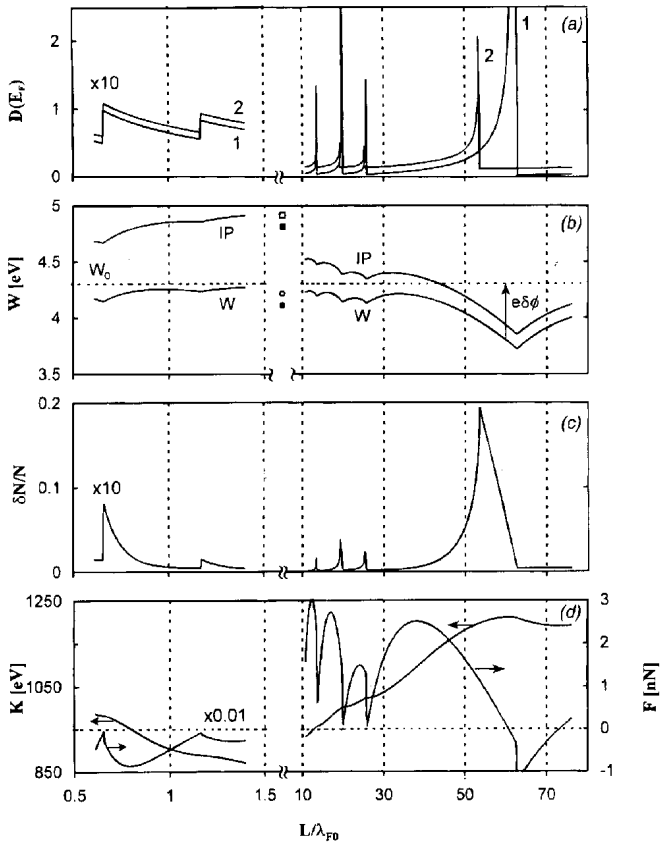

Fig. 1. Characteristics of the elongated sample as functions of the length (in units of L/λ_{F0}, where λ_{F0} is the Fermi wave length of the reservoir, $\lambda_{F0} = 2\pi/k_{F0}$). The left side of the figure corresponds to a slab while the right one to a wire. a — density of states at the Fermi level of an isolated specimen (*1*) and a specimen in a contact (*2*). b — the work function, ionization potential, and CPD of an isolated slab and a wire. For comparison, the values of W (○, ●) and IP (□, ■) for a rigid (upper points) or self-compressed (lower points) spherical cluster of volume 4 nm^3 [32] are placed "between" the slabs and wires. c — the size-dependent part of the number of electrons spilling out from the specimen in a contact with reservoirs. d — total kinetic energy K of the electrons (left axis) and elongation force F (right axis) of the isolated specimen

single-electron devices [28]. Then, assuming that $C_c = e\delta N/\delta\phi$, $\delta N \ll N$ and $\Delta \to 0$, Eq. (15) yields

$$\delta\phi = (W_0 - W)/e > 0. \tag{16}$$

For example, the energy spectrum E_{n1_x} of the remaining electrons in the slab, $N_1 = N - \delta N$, can be found by solving (4) for a square potential well of depth

$$U_1 = U - e\delta\phi, \tag{17}$$

where U corresponds to the isolated slab. Comparing (17) with (1) and using (16) we find that, in equilibrium between a specimen and the electrodes, the magnitude of E_{F1} is equal to that of an isolated specimen (E_F). The value of δN can be calculated using Eq. (8) with the change $N \to N_1$ and $k_{n_x} \to k_{n1_x}$. The total kinetic energy, K_1, of the remaining electrons is defined as earlier (Eq. (12)) with the changed energy spectrum and number of electrons. The same approach was used for a nanowire. In the case of an open system, the elastic force is determined by a surplus pressure, relative to the reservoirs, multiplied by the area of the contact:

$$F_1 = -\frac{d\Omega}{dL}, \tag{18}$$

where the size-dependent part of the grand potential Ω is given by

$$\Omega = E_1 + W_0 N_1, \tag{19}$$

and $E_1 = -K_1$.

3. Results and Discussion

The calculations were performed for the set of isolated Au slabs and wires and then for the ones in contact with reservoirs. It allowed us to calculate the contact potential which is needed for the force characteristics. Assuming the ideal plastic deformation in the experiments [1, 10], the volume of a deformed specimen will be constant. All considered specimens have the same volume, $V = 4$ nm^3, and the number of electrons $N = 236$. The linear sizes of a specimen vary in the range: $\sqrt{\pi} r_s < L < 13a_0$ for slabs, and $L_0/10 > a > \sqrt{\pi} r_s$ for wires. Here, $a_0 = \hbar^2/me^2$ is the Bohr radius. The calculated energy and force characteristics corresponding to a slab and a wire, respectively, are displayed on the left and right parts of Figs.1 and 2. The wire length, $L = L_0 + \Delta L$, has been increased by about seven times.

Fig. 1,*a* shows the density of states, $D(E_F)$, of an isolated specimen (curve *1*) and the one contacted with reservoirs (curve *2*) versus the wire length. For a better demonstration, curves *2* are slightly shifted up. The peaks of the $D(E_F)$ for a wire with square cross-section are more intensive for the additionally degenerate subband, $k_{n_y} = k_{n_z}$.

Fig. 1,*b* displays the behavior of the electron work function and the ionization potential of the isolated specimens of varying size. The potential difference $\delta\phi$ that arises at the contact is also indicated. The inequality $W(L) < W_0$ is observed to be obeyed over the whole range of the considered lengths of the slab

and wire. In the shortest wire, five subbands appear and four of them disappear at elongation. The amplitudes of oscillations of the Fermi level are of one or two tenths of eV. They are substantially less than those calculated self-consistently for the extended thin Al slabs [29] and wires [30, 31]. As can be seen, there are the ranges of widths, where IP$< W_0$ and IP$> W_0$. The fact that IP$< W_0$ is rather unexpected. Judging from the empirical fact that the work function W_0 of the alkali metal is approximately equal to one half of the IP of an atom, one would expect that the IP of a small solid (independently of the shape of its surface) falls in the range $W_0 <$ IP(cluster) $<$ IP(atom).

The size correction in $W(L)$ competes with the $e^2/2C$ term in expression (10) for the ionization potential. The magnitude of IP(L) depends on the shape of a specimen: IP$(L) > W_0$ for $L < 43\lambda_{\mathrm{F0}}$ and IP$(L) < W_0$ for $L > 43\lambda_{\mathrm{F0}}$. Note that the positions of local minima in the $IP(L)$ and $W(L)$ curves correspond to the positions of the peaks in the density of states of an isolated specimen (Fig. 1,*a*). In the case $a = L$, we deal with a metal cube whose ionization potential must have a value similar to that of a sphere. It should be noted that the ionization potential depends only on the geometry of the specimen and is independent of the direction of electron emission [21, 22].

The CPD leads to a noticeable negative shift of the potential well depth (at the utmost point by about 0.5 eV) and this leads, in turn, (Fig. 1,*a*) to a shift in the density of states (curve *2*) to the zone of a bigger cross section.

Fig. 1,*c* shows the size dependence of the number of electrons δN that have left the specimen. An increase in the cross section or a decrease in the wire length leads to the breaks appearing in the monotonic components of $\delta\phi(L)$ and $\delta N(L)$ which correspond to a spherical specimen. For a close to the atomic diameter, the δN makes up 20% of the initial number of electrons. The account for the contact potential leads to a dependence of δN on the hierarchy of energy levels in an isolated specimen. This aligns specific breaks in the $\delta N(L)$ curve which shows the positions of the peaks in the density of states $D(E_{\mathrm{F}})$ of both isolated and contacted specimens. The results show that some part of the electrons is spilled out from the slab (wire) in a contact and the contact can be thought of as a sort of the "electron pump" which pulls out the electron liquid from or draws it into reservoirs. The dipole layers formed in a vicinity of both contacts must stimulate an additional longitudinal deformation of the wire and contribute to a change in its shape and

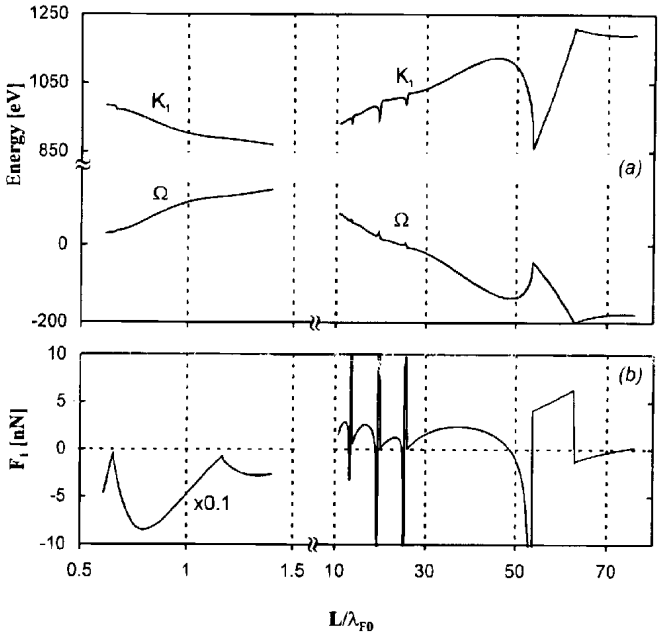

Fig. 2. Total kinetic energy K_1, grand potential Ω, and elastic force F_1 of an elongated slab and a wire in a contact

in the electron density. The above results allow us to calculate the size dependence of the effective capacitance $C_c = e\delta N/\delta\phi$ for a specimen in contact.

The kinetic energy of electrons and the elongation force of an isolated specimen are displayed in Fig. 1,*d*. Their counterparts for the specimen after the junction with reservoirs as well as the potential Ω are shown in Fig. 2. The total electron kinetic energy $K(L)$ and $K_1(L)$ of a metal cube are similar to those for a semiinfinite metal, $(3/5)NE_{\mathrm{F0}}$.

The amplitudes of force oscillations $F(L)$ of an isolated slab are several times bigger than those measured for nanowires [1, 10]. It is stipulated by a large value of the cross section $a \times a$. Nevertheless, dividing the first amplitude of the force by the number of atoms in the slab, one gets 0.4 nN. This value is smaller than the force acting on a single atom (1.6 nN) in the point contact experiments [1, 10]. That can be explained by the different dimensionalities of a slab and a wire. For the reduced dimensionality, the amplitudes of force oscillations range from 1 to 3 nN, which is similar to the measured values. The character of the dependence $F(L)$ changes significantly at the wire contact because of a depletion of the electron subsystem and due to a shift of the spectrum. It should be mentioned that, in our approach, the size dependences $K(L)$ and $K_1(L)$ are qualitatively different from those obtained for an

infinitely deep potential well [2, 3, 6]. The second term appearing in (19) only partly levels the oscillations in $\Omega(L)$. This is in contrast to the infinitely deep potential well, where the oscillations in $\Omega(L)$ disappear. As a result, the amplitudes of force oscillations $F_1(L)$ and their shape change significantly. In our more advanced model, the attempt to take into account CPD leads to the appearance of spikes in the elastic force versus length, which results from the fact that, for the isolated and contacted wires, the densities of states are not in line. It is possible that, in experiment, these peaks could not be recognized against the background of thermal fluctuations of the wire form which occur during deformation. With the exception for the interval $54 < L/\lambda_{F0} < 62$ (Fig. 2,*b*), the calculated amplitudes of force oscillations agree with the experimental values. The difference may be stipulated by a not self-consistent determination of CPD for the wires whose diameter is comparable with the atomic dimensions and by the supposed continuous variation in L . Another reason might be that the elastic force is sensitive to the applied voltage as suggested in [33, 34].

The choice of a simplified form of the wire and a non self-consistent treatment of the size oscillations in the potential U are the disadvantages of the model. The free-electron model is not able to describe the effect of atomic rearrangements on the magnitude of force at the atomic contact [10] in detail. On the other hand, the obtained qualitative results are quite general and should not depend on the symmetry of the problem. It should be also noted that, for the stabilized jellium model, the bulk modulus [22, 35], work function, surface energy, and surface stress [21, 22] for gold can be described only when its valency is assumed to be three. The transition from monovalent to trivalent gold can lead to the increased, by several times, amplitude of oscillations of the elastic force in analogy with that observed for the trivalent Al [14]. These problems can be connected with the unusual size dependence of IP(R) that is measured for spherical gold particles: for very large particles as well as for the atomic-size ones IP$> W_0$, whereas IP$< W_0$ for particles with intermediate R [37, 38]. In our view, this could be explained by a reduced valency of some metals, which is connected with decreasing the size of a specimen (it reminds the metal-nonmetal transition). A similar transition was observed [39] for mercury clusters and interpreted in [40]. The behavior of the ionization potential measured for aluminum clusters (compare Fig. 28,*a* in [41]) also points to this effect. Therefore, the assumption of monovalency of Au in low-dimensional structures is quite reasonable.

Finally, we would like to point to the connection between our results and the famous phenomenon of the quantization of the shear modulus for polycrystalline specimens that was experimentally observed for 57 elements at room temperature [42]. Possibly, this effect may be explained by the quantization of the force characteristics of the $2D$ electron liquid in the intercrystallite space of a polycrystal.

The results of this paper can be summarized as follows. The evolution of the size dependence of the ionization potential during the transformation of the shape of a specimen from a slab to a wire is investigated. The size dependence of CPD is calculated in a simple manner. It is shown that the infinite potential well model of a slab [8] overestimates the value of CPD by many times. For the first time, the effect of CPD on the size oscillations of force was demonstrated. The magnitude of the calculated CPD is significant for the wires of subatomic diameters only. An analytic expression for the dependence of the potential well depth on the Fermi energy for a semiinfinite metallic system is tested for low-dimensional structures. [Remarks: Notwithstanding that the expressions derived in [15—18] successfully describe the character of the behavior of the electron work function (of positive value) for semiinfinite metals and ionization potentials for metallic clusters, in our view, a usage of the classical electrostatics concept (image force) to define the quantum characteristic — work function — is not fully appropriate because it cannot unequivocally determine the sign of the emitted particle. For example, the positron work function is positive for sodium and negative for aluminum in spite of the identical action of the image force on this particle [43].]

The work of one of the authors (V.V.P.) during his stay in Wrocław was supported by the Mianowski Fund (Poland) and partially by the Ministry of Education and Science of Ukraine.

1. *Rubio G., Agraït N., Vieira S.*// Phys. Rev. Lett.—1996.— **76**.— P.2302—2306.
2. *Van Ruitenbeek J. M., Devoret M. H., Esteve D., C. Urbina C.*// Phys. Rev. B.— 1997.— **56**.— P.12566—12572.
3. *Stafford C. A., Baeriswyl D., Bürki J.*// Phys. Rev. Lett.— 1997.—**79**.— P.2863—2869.
4. *Yannouleas C., Landman U.*// J. Phys. Chem. B.— 1997.— **101**.— P.5780—5788.
5. *Yannouleas C., Bogachek E.N., Landman U.*// Phys. Rev. B.— 1998.— **57**.— P.4872—4881.
6. *Blom S., Olin H., Costa-Kramer J.L. et al.*// Ibid.— 1998.— **57**.— P.8830—8835.
7. *Tomchuk P.M.*//Ukr. Fiz. Zh.— 2002. — **47**, N 9. — P.833—841.

8. *Moskalets M.V.*// Pis'ma Zh. Exp. Teor. Fiz.— 1995.— **62**— P.702—704 [JETF Lett.—1995.—**62**.— P.719—721].
9. *Brandbyge M., Schiøtz J., Sørensen M.R. et al.*// Phys. Rev. B.— 1995.—**52**.–P.8499—8512.
10. *Rubio-Bollinger G., Bahn S.R., Agraït N. et al.*// Phys. Rev. Lett.— 2001.— **87**.— 026101(4).
11. *Ekardt W.*// Phys. Rev. B.— 1984.— **29**.— P.1558—1570.
12. *Rogers III J. P., Cutler P. H., Feuchtwang T. E., Lucas A. A.*// Surf. Sci.— 1987.— **181**.— P.436—446.
13. *Pogosov V. V.*// Solid State Communs.— 1990.— **75**.— P.469—474.
14. *Pogosov V.V., Kotlyarov D.P., Kiejna A., Wojciechowski K.F.*// Surf. Sci.— 2001.— **472**.— P.172—179.
15. *Halas S., T. Durakiewicz T.*// J. Phys.: Condens. Matter.— 1998.— **10**.— P.10815—10824.
16. *Brodie I.*// Phys. Rev. B.— 1995.— **51**.— P.13660—13667.
17. *Durakiewicz T., Arko A.J., Joyce J.J., Moore D.P., Halas S.*// Surf. Sci.— 2001.— **478**.— P.72—82.
18. *Wong K., Vongehr S., Kresin V.V.*// Phys. Rev. B. — 2003. — **67**. — 035406.
19. *Fomenko V.S., Podchernyaeva J.A.* Emission Properties of Materials. — Moscow: Atomizdat, 1975 (in Russian).
20. *Harrison P.* Quantum Wells, Wires and Dots: Theoretical and Computational Physics. — Chichester, UK: Wiley, 1999.
21. *Pogosov V.V., Kurbatsky V.P.*// Zh. Exper. Teor. Fiz.— 2001.— **119**.— P.350—360 [JETF.—2001.—**92**.— P.304—314].
22. *Pogosov V.V., Shtepa O.M.*// Ukr. Fiz. Zh.— 2002.— **47**, N11.— P.1065—1071.
23. *Landau L.D., Lifshitz E.M.* Electrodynamics of Continuous Media. - New York: Pergamon, 1960.
24. *Vasil'ev B.V., Lyuboshits V.L.*// Uspekhi Fiz. Nauk.—1994.— **164**.—P.367—389.
25. *Ziesche P., Gräfenstein J., Nielsen O.H.* // Phys.Rev. B.— 1988.—**37**.—P.8167—8178.
26. *Iakubov I.T., Khrapak A.G., Podlubny L.I.et al.*// Solid State Communs.—1985.— **53**.— P.427—433.
27. *Perdew J.P.*// Phys. Rev. B.—1988.— **37**.— P.6175—6185.
28. *Likharev K.K.*//Proc. IEEE.— 1999.— **87**.— P.606—632.
29. *Sarria I., Henriques C., Fiolhais C., Pitarke J.M.*// Phys. Rev. B. — 2000.— **62**.— P.1699—1707.
30. *Zabala N., Puska M.J., Nieminen R.M.*// Ibid.— 1999.—**59**.— P.12652—12659.
31. *Puska M.J., Ogano E., Zabala N.*// Ibid.— 2001.— **64**.— 033401(6).
32. *Kiejna A., Pogosov V.V.*// J. Phys.: Condens. Matter.— 1996.— **8**.— P. 4245—4257.
33. *Zagoskin A.M.*// Phys. Rev. B.— 1998.— **58**.— P.15827—15832.
34. *Brandbyge M., Mozos J.-L., Ordejon P. et al.*// Ibid.— 2002.— **65**,16.— 165401 (18).
35. *Wojciechowski K.F.*// Physica. B.— 1996.— **229**.— P.55—61.
36. *Kiejna A., Wojciechowski K.F.* Metal Surface Electron Physics. — Oxford: Pergamon, 1996.
37. *Garron R.*// Ann. Phys.— 1965.— **10**.— P.595—625.
38. *Borzyak P.G., Katrich G.A., Samoilov V.S.* // Dispersed Metallic Films. — Kyiv: Nauk. Dumka, 1976 (in Russian).— P.90.
39. *Rademann K., Kaiser B., Even U., Hensel F.*// Phys. Rev. Lett.— 1987.— **59**.— P.2319—2324.
40. *Garcia M.E., Pastor G.M., Bennemann K.H.*// Ibid.– 1991.— **67**.— P.1142—1147.
41. *de Heer W.A.*// Rev. Mod. Phys.— 1993.— **65**.— P.611—676.
42. *Bell J.F.* Encyclopedia of Physics / Chief Ed. S. Flügge. — Vol. VIa/1; Mechanics of Solids / Ed. C. Truesdell.— (Berlin: Springer-Verlag, 1973. [in Russian, J.F.Bell Experimental Backgrounds of Deformed Solids Mechanics, Part I Small Deformations (Moskow, Nauka, 1984) P.505].
43. *Pogosov V.V., Iakubov I.T.*// Fiz. Tverd. Tela.—1994.— **36**.— P.2343—2353. [Phys. Solid State.— 1994.— **36**.— P.1274—1284].

Received 18.03.03

ПРОСТА МОДЕЛЬ ЕНЕРГЕТИЧНИХ І СИЛОВИХ ХАРАКТЕРИСТИК МЕТАЛЕВИХ НАНОКОНТАКТІВ

В.В.Погосов, В.П.Курбацький, Д.П.Котляров, А.Кієна

Р е з ю м е

Квантові осциляції енергетичних характеристик і пружної сили ізольованих і приведених у контакт з електродами золотих пластинок і дротиків розраховано в моделі вільних електронів і потенціальної ями скінченної глибини. Використано і тестовано просте співвідношення між енергією Фермі і глибиною потенціальної ями для низьковимірних структур. Показано, що електронну підсистему зразка, приведену в контакт, слід розглядати як відкриту. Контакт діє як своєрідний електронний насос, втягуючи і виплескуючи електрони із зразка. Досліджено вплив контактної різниці потенціалів на осциляції пружної сили пластинки і дротика. Розраховані значення амплітуди осциляцій сили задовільно узгоджуються з експериментальними.